Research Article ISSN 2771-666X

Journal of Advanced Materials Science and Engineering

The Use of a Suspension of Functionalized Gadolinium Oxide Nanoparticles for Photocatalytic Applications

Massard C* and Awitor K.O

Université Clermont Auvergne, Equipe PCSN (IUT Clermont Auvergne), Laboratoire de Physique de Clermont UMR 6533, CNRS/IN2P3, F-63000 Clermont-Ferrand, France.

***Correspondence:**
Massard C, Institut Universitaire de Technologie, Equipe de recherche PCSN, Université Clermont Auvergne, CNRS/IN2P3, Laboratoire de Physique de Clermont UMR 6533, F-63000 Clermont-Ferrand, France.

Received: 16 Mar 2022; **Accepted:** 19 Apr 2022; **Published:** 25 Apr 2022

Citation: Massard C, Awitor KO. The Use of a Suspension of Functionalized Gadolinium Oxide Nanoparticles for Photocatalytic Applications. J Adv Mater Sci Eng. 2022; 2(1): 1-8.

ABSTRACT

Photo-degradation of Rhodamine B (RhB) in aqueous solution was use as a probe to assess the photocatalytic activity of Gadolinium oxide (Gd_2O_3) nanoparticles in suspension under UV irradiation. The nanoparticles in suspension were prepared by a polyol method using gadolinium chloride hexahydrate ($Gd_2Cl_6.6H_2O$) and diethylene glycol (DEG) as starting precursors. The physico-chemical properties of the elaborated suspension are analyzed using X-ray diffraction (XRD), ultraviolet visible (UV-vis) and infrared (FTIR) spectroscopies, transmission electron microscopy (TEM) and viscosimetry. The Gd_2O_3 nanoparticles in suspension were used as photocatalyst for the degradation of Rhodamine B (RhB) dye under irradiation with UV light. The results of the kinetic studies showed that the photodegradation reactions were followed by a pseudo first order reaction rate law over the first 30 minutes of monitoring. The elaborated Gd_2O_3 nanoparticles suspension showed a great efficiency in the photocatalytic test without any addition of a co-catalyst, thus limiting the complexity of the further decontamination process of waste water.

Keywords

Gadolinium oxide nanoparticles, Photocatalysis, Kinetic study, Viscosimetry.

Introduction

The research theme on nanomaterials is increasingly evolving with several thousand research articles published each year [1]. The extremely small dimensions of these nanomaterials give them unique properties that open the way to many applications from energy storage [2-3] to biochemical engineering applications [4]. Among all the forms that nanomaterials can take, nanoparticles are in the forefront such as in dentistry applications [56], depollution of the environment [7-8], sustainable agriculture [9-10], optical components [11-12] and nanomedicine [13-14]. A civilizational issue concerns the fight against organic pollutants on a global scale [15] including the depollution of wastewater which requires the implementation of remediation processes [16-17]. The textile industry generates large volumes of wastewater, polluted with organic dyes, leading to high carcinogenic risks when the contaminants are dispersed in ecosystems [18-19]. Water depollution can be achieved by means of photocatalytic reactions induced by the irradiation of a semiconductor metal oxide [20-21]. Lanthanides, thanks to their particular electronic configuration and their energy gap, are interesting candidates for the photocatalytic depollution of polluted waters [22-23]. In the lanthanide group, gadolinium oxide is used as a semiconductor photocatalyst [24-25]. Concerning the photocatalytic reaction of organic dye in wastewater, gadolinium oxide is often used together with the addition of oxygen peroxide as co catalyst, a process called advanced combined oxidation (AOP) [26-27]. In this study, we demonstrate that the synthesized Gd_2O_3 suspension can be used successfully for the photocatalytic degradation of Rhodamine B complexity of the decontamination process.

Experimental Section

Materials

The following analytical-grade reagents were used without further purification:

Gadolinium (III) chlorate hexahydrate (99.9%) and diethylene glycol (99%) were purchased from Alfa Aesar. Sodium hydroxide pellets (99%) were purchased from VWR international.

Synthesis of gadolinium oxide nanoparticles in suspension

In order to produce the gadolinium oxide (Gd_2O_3) core of the nanoparticles, a polyol synthesis was used [28-29]. Firstly, $Gd_2Cl_6.6H_2O$ was dissolved in diethylene glycol (DEG) by using magnetic stirring and heating to reflux for 3 hours. Secondly, to this colorless solution, concentrated sodium hydroxide solution (10 M) was added drop by drop. This addition causes the formation of a white precipitate. Thirdly, the resulting mixture is then heated to reflux under magnetic stirring for 5 hours. After these 5 hours of treatment, the white precipitate has disappeared and the mixture becomes a clear suspension. The last step of the synthesis consists in a return to room temperature by maintaining a magnetic stirring during 15 hours. A stable suspension of gadolinium oxide nanoparticles in diethylene glycol is obtained.

Transmission Electron Microscopy (TEM)

The TEM image of the Gd_2O_3 suspension sample is obtained using a Hitachi transmission electron microscope (H7650). The accelerating voltage used was 80 kV. Picture was taken using a Hamamatsu AMT CCD camera placed in a side position. To perform the characterization, 10 µL sample solution was deposited on a 300-mesh carbon-coated copper grid and dried at room temperature.

X-ray diffraction spectroscopy (XRD)

The XRD measurement was performed using a Bruker D2 Phaser diffractometer. The pattern was recorded by CuKα1 radiation with λ of 1.5406 Å and nickel monochromator filtering wave at tube voltage of 30 kV and tube current of 10 mA. The scanning was done in the region of 2θ from 20° to 60°. The size of the nanoparticles was calculated using the Scherrer's formula.

UV spectroscopy

The UV-vis spectra of the suspensions of gadolinium oxide nanoparticles were recorded using a Jenway 7310 single beam UV-vis spectrophotometer from 300 to 700 nm. Ultra-pure water was taken as reference for the photocatalytic measurement whereas diethylene glycol is used for the blank for the Gd_2O_3 suspension alone.

FTIR spectroscopy

The spectrum was obtained using a Perkin Elmer Spectrum one Fourier Transform Infrared (FTIR) spectrometer in transmission, with the KBr pellet method.

Dynamic viscosity measurements

The dynamic viscosity of the suspension of gadolinium oxide nanoparticles in diethylene glycol was measured using a Brookfield DV2T programmable viscosimeter connected to a Julabo temperature-controlled bath as shown in Figure 1. The DV2T viscosimeter drives a spindle immersed in the tested fluid through a calibrated spring. The viscous drag of the fluid against the rotating spindle was measured by the deflection of the calibrated spring and recorded by a rotary transducer. An amount of 16 mL was used in the measurement. The fluid sample was filled into the water jacket specialized for the measurement of low viscosity. The cylinder water jacket was connected to the ULA (Ultra Low Adapter). The water jacket was attached to the viscosimeter. The water bath maintains the sample temperature in the range 20-80°C. The temperature of the sample is measured using the thermocouple connected with the viscosimeter. The fluid sample was heated up to reach as table temperature before the viscosity measurement. The spindle rotation speed is selected to ensure that the applied torque was set between 10% and 100%. Within this torque range, the instrument produced satisfactory result. The viscosimeter is connected to a computer which records the data automatically. The Rheocalc T 1.2.19 software is used to treat the experimental data such as spindle rpm, viscosity, temperature, shear stress, shear rate, torque % and time.

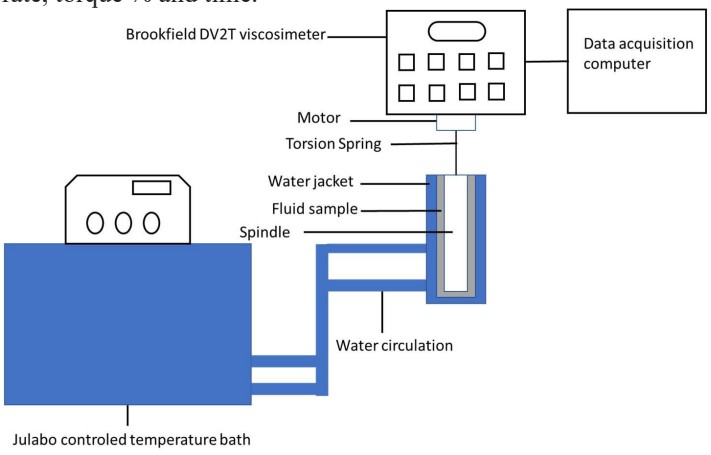

Figure 1: Experimental set-up for viscosity measurement of the suspension.

Results and Discussion

Transmission electronic microscopy (TEM) characterization

Figure 2 shows a high magnification TEM image of the Gd_2O_3 nanoparticles in suspension prepared with NaOH as alkaline source. This panoramic image of the as-prepared Gd_2O_3 sample clearly exhibiting that the sample is entirely composed of small and relatively uniform spherical nanoparticle with diameter of 2-6 nm. It can be seen that the suspension of well dispersed nanoparticles with a spherical morphology.

X-ray diffraction characterization

The XRD spectrum of the synthesized Gd_2O_3 nanoparticles is shown in Figure 3. The main diffraction peaks are positioned at 2θ =27.26°, 31.59°, 42.36° and 57.21° are closely matched with to the (222), (400), (134) and (622) crystal planes of the Gd_2O_3 cubic phase published by the Joint Committee on Powder Diffraction Standards (JCPDS) N° 43-01014 data card. These experimental data also coincide well with other previous published data [30-31].

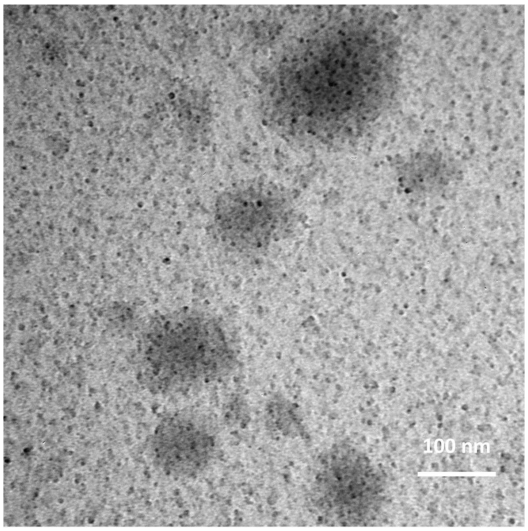

Figure 2: TEM micrograph of Gd_2O_3 nanoparticles in suspension prepared with NaOH as alkaline source.

The interplanar distance d is calculated from the Bragg equation:

$$\lambda = 2d \sin\theta \ (1)$$

Based on the (222) crystal plane of Gd_2O_3, the interplanar distance was equivalent to 3.269 Å which is in goof agreement with previous studies [32].

The particle size of the Gd_2O_3 nanoparticles was determined by the X-ray line broadening method using the Scherrer equation [33]:

$$D = \frac{K\lambda}{\beta \cos\theta} \ (2)$$

where D is the particle size in nanometers, λ is the wavelength of the radiation (1.54056 Å for CuKα radiation), k is a constant equal to 0.94, β is the peak width at the half-maximum intensity and θ is the Bragg diffraction angle. We calculated the crystallite size by using the FWHM of the Gd_2O_3 (400) peak. From the calculation, it was found that the Gd_2O_3 nanoparticle had a crystallite size in the range of 2.4 nm which is in a good agreement with the TEM image considering possible aggregation during sampling for microscopic analysis.

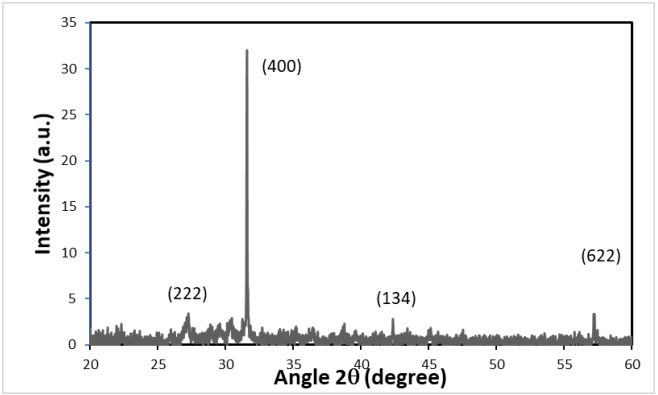

Figure 3: XRD pattern of the synthesized Gd_2O_3 nanoparticles in suspension.

UV-vis spectroscopic analysis

The Gd_2O_3 suspension was analyzed using UV-vis spectroscopy. The UV-vis spectrum of the suspension was displayed in Figure 4. The maximum absorbance of the Gd_2O_3 nanoparticles was found under the 300 nm wavelength, near 230 nm wavelength [34].

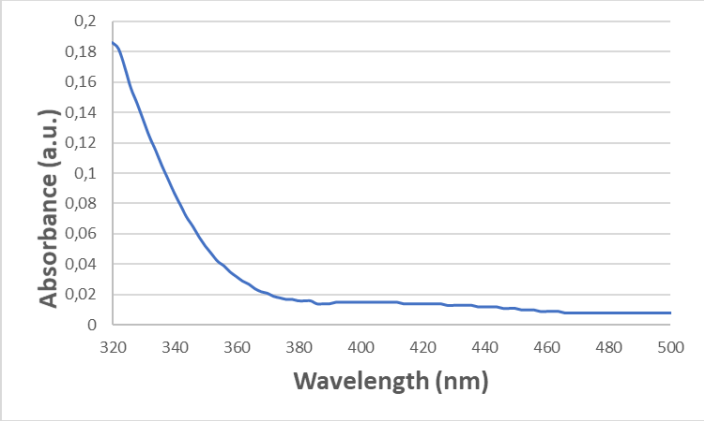

Figure 4: UV-vis spectrum of the Gd_2O_3 nanoparticles suspension.

FTIR spectroscopic analysis

The Gd_2O_3 nanoparticles were analyzed using FTIR spectroscopy. The FTIR spectrum was displayed in Figure 5. On this spectrum, the band at 547 cm^{-1} can be assigned to the Gd-O stretching frequency of Gd_2O_3 [35]. This result is in good agreement with the XRD pattern revealing the presence of Gd_2O_3.

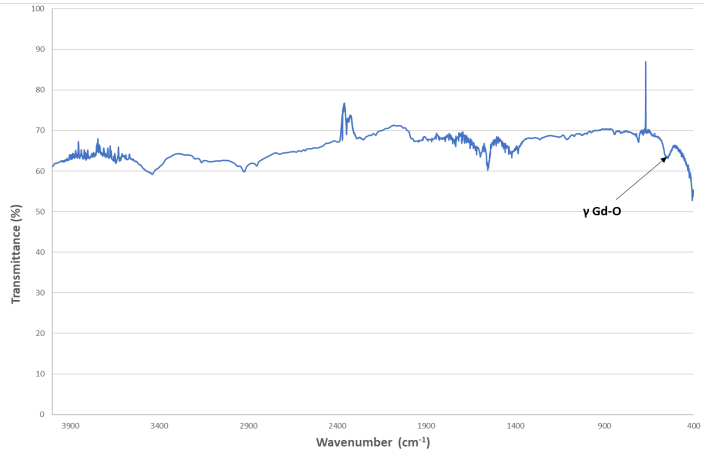

Figure 5: FTIR spectrum of the Gd_2O_3 nanoparticles.

Dynamic viscosity measurements

In order to verify the analysis setup, dynamic viscosity measurements are performed on the diethylene glycol as a function of temperature. The data obtained are compared with those that have been published [36]. The experimental values match nicely with the published data, see Figure 6. The maximum difference is of ± 3 % between the experimental data and the published ones, with the temperature ranging from 30 to 60°C.

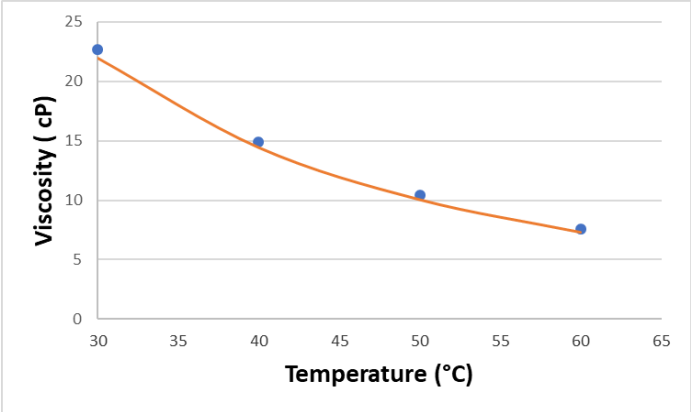

Figure 6: Comparison of published viscosity values (line) and experimental data (dots) for diethylene glycol.

Figure 7 shows shear stress (dyne/cm^2) versus shear strain rate (s^{-1}) for the Gd_2O_3 suspension at 20°C. The suspension clearly exhibits a Newtonian behavior. Since the carrying liquid of the nanoparticles exhibits a Newtonian behavior, it seems that the rheological property of the liquid dominates the whole mixture if the nanoparticle concentration is not high enough to modify the viscous properties [37].

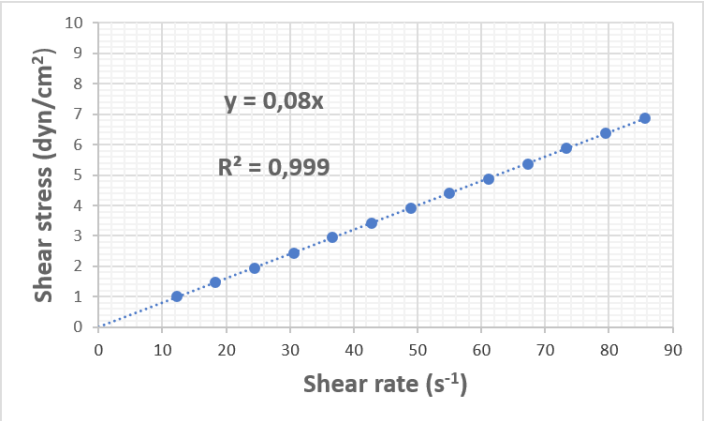

Figure 7: Shear stress (dyne/cm^2) versus shear rate (s^{-1}) for the Gd_2O_3 suspension at 20°C.

Viscosity measurements of the Gd_2O_3 suspension were carried out with varying temperature between 25 and 40°C. The results are shown in Figure 8. Analysis of this data indicates an exponential decrease of the viscosity with the increase of the temperature. This general trend was observed repeatedly in viscosity measurements as a function of temperature for nanofluids [38-39].

All these rheological tests show the stability and the good dispersion of gadolinium oxide nanoparticles in the carrier liquid. This stability is very important to optimize the photocatalysis of the photodegradation reactions of organic compounds which occur on the surface of the nanoparticles and which requires a maintenance of their individualization in order to maximize the number of active sites.

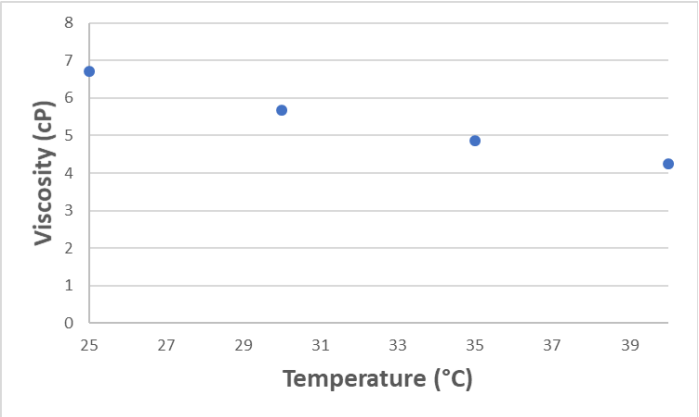

Figure 8: Experimental values of the viscosity of Gd_2O_3 suspension with respect to sample temperature.

Photocatalytic degradation of Rhodamine B dye using Gd_2O_3 nanoparticles in suspension

The histogram of photocatalytic degradation of Rhodamine dye under various conditions is shown in Figure 9. It can observe from the histogram that the adsorption of the dye Gd_2O_3 nanoparticles is negligible as it represents about 1% at the end of one hour of contact without irradiation. Secondly, the irradiation of the Rhodamine B solution without the nanoparticles leads to only a small value of the photocatalytic efficiency, after one hour of UV (Figure 9), the dye degradation process is very slow and limited. Finally, the histogram shows that the joint use of Gd_2O_3 nanoparticles and UV irradiation considerably accelerates the degradation process, after only 30 minutes of UV light exposure, the photocatalytic degradation efficiency is the highest, as it reaches 30% unlike to some works involving doping processes [40-41] or co-catalyst addition [42].

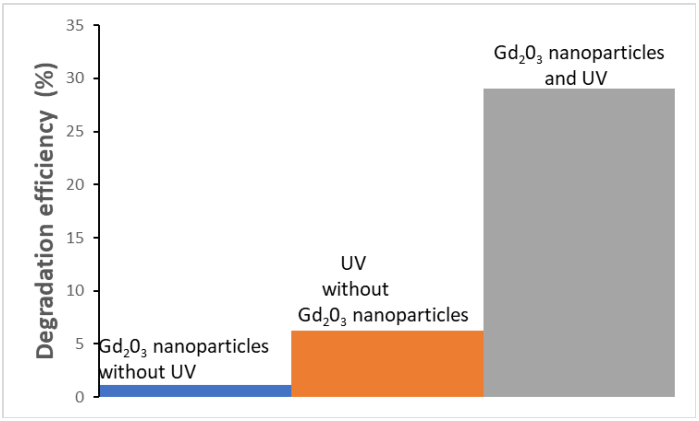

Figure 9: Histogram of photocatalytic degradation efficiency under different conditions.
(Experimental conditions: initial dye concentration: 2.4 ppm, wavelength of UV irradiation:
254 nm, dye volume: 5 mL photocatalyst volume: 5 µL).

The aqueous solution of Rhodamine B containing the Gd_2O_3 nanoparticles showed the classical absorbance peak at 552 nm [43-44]. The intensities of maximum absorption peak at 552 nm continuously decrease with the increase of UV light exposure time

showing the progressive degradation of the Rhodamine B dye, see Figure 10.

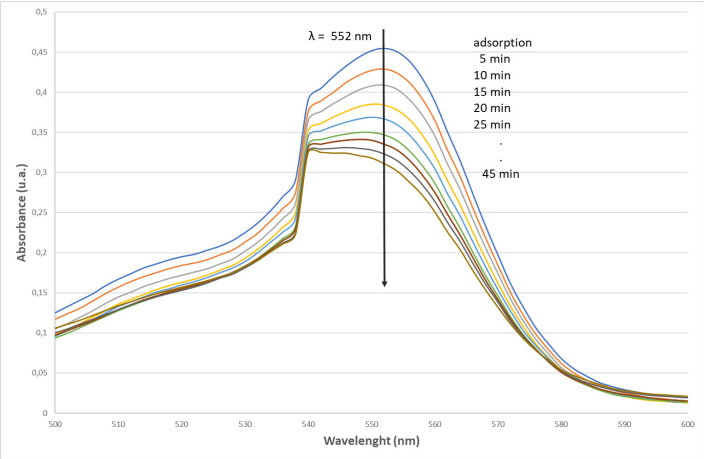

Figure 10: UV-VIS absorption spectra of photocatalytic degradation of the Rhodamine B dye.
(Experimental conditions: initial dye concentration: 2.4 ppm, wavelength of UV irradiation:
254 nm, dye volume: 5 mL photocatalyst volume: 5 µL).

The photodegradation process of the Rhodamine B dye catalyzed over the surface of the synthesized Gd_2O_3 nanoparticles occurred with short irradiation times, in the absence of cocatalyst and with low UV power densities. This result validates the use of the synthesized gadolinium oxide nanoparticles suspension as a high efficiency photocatalyst for the implementation of simple and efficient wastewater treatment processes.

Kinetic study for photocatalytic degradation of Rhodamine B dye

Considering the photocatalytic degradation of Rhodamine B as a first-order reaction:

$$[RhB] \rightarrow Products$$

The rate (v) of the reaction is expressed as follows:

$$v = -\frac{d[RhB]}{dt} = k[RhB] \quad (3)$$

Where [Rh*B*] is the Rhodamine B concentration, k the first order rate constant and t is the time.
After separation of the variables we obtain

$$-\frac{d[RhB]}{[RhB]} = kdt \quad (4)$$

$$\int_{[RhB]_0}^{[RhB]} \frac{d[RhB]}{[RhB]} = -\int_{t_0}^{t} kdt \quad (5)$$

And finally, by integration

$$\ln\left(\frac{[RhB]}{[RhB]_0}\right) = -k \times t \quad (6)$$

Where [RhB] is the Rhodamine B at an initial time t_0, [RhB] is the Rhodamine B concentration at a specific time t and k is the first order rate constant. The experimental results obtained confirm that the photodegradation reaction of rhodamine assisted by the nanoparticle suspension follows a pseudo first-order reaction rate law as reported in previous work [45-46]. From Figure 11, the values of the determination coefficient (R^2) for the pseudo first-order reaction kinetics are 0.9856 using Gd_2O_3 nanoparticles

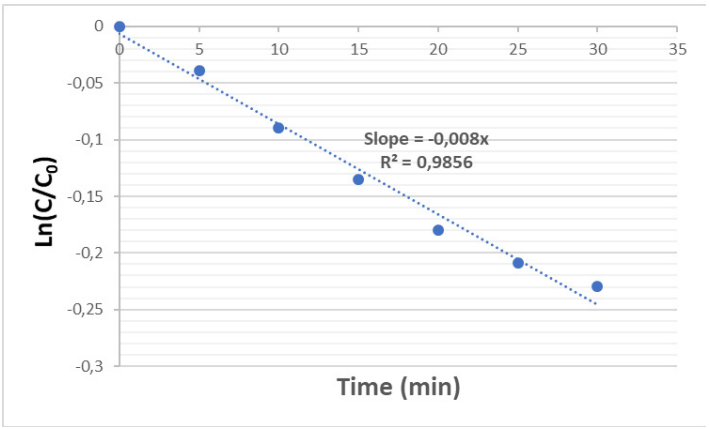

Figure 11: Kinetic study of the photodegradation reaction of Rhodamine B assisted by the Gd_2O_3 nanoparticle suspension. (Experimental conditions: initial dye concentration: 2.4 ppm, wavelength of UV irradiation: 254 nm, dye volume: 5 mL photocatalyst volume: 5 µL).

Concerning the mechanism pathway, the photodegradation reaction of rhodamine belongs to the category of the advanced oxidative process (AOP) [47-48]. AOPs are associated with various reactive oxygen species (ROS), such as hydroxyl radical (·OH). Under UV irradiation, the electrons present in the valence band of the gadolinium oxide pass into the conduction band see Figure 12. Electron-hole pairs are thus continuously generated, which ensures the activity of the gadolinium oxide. Holes with a high oxidative power are able to absorb on water molecule which forms a radical species (·OH). On the surface of the nanoparticles, the radicals act as oxidizing agents on the azo dye molecules [49].

$$Gd_2O_3 + hv \rightarrow Gd_2O_3(e_{cb}^- + h_{vb}^+) \quad (7)$$

$$Gd_2O_3(h_{vb}^+) + H_2O \rightarrow Gd_2O_3(\bullet_{OH}) + H^+ \quad (8)$$

OH + RhB → intermediate products → degraded products (9)

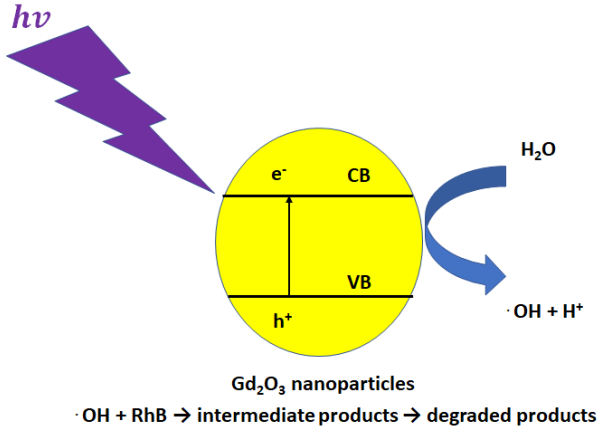

Figure 12: Possible mechanism of photocatalytic degradation of Rhodamine B dye by Gd_2O_3 nanoparticles. CB: Conduction Band, VB: Valence Band. e^-: Electron; h^+: hole.

It seems that the electrons present in the conduction band generate a superoxide radical · O which is not involved in the degradation process [50-51].

$$Gd_2O_3(e_{cb}^-) + O_2 \rightarrow \cdot O_2^- + Gd_2O_3 \quad (10)$$

Only the hydroxide radicals and the holes participate effectively in the degradation process of the azo compound.

Conclusion

In this study, we have demonstrated the relevance of using a gadolinium nanoparticle suspension as a photocatalytic substance using Rhodamine B to simulate an organic pollutant present in wastewater. We highlight in our case that the degradation reaction does not require any cocatalyst or complex alloy. In order to better define the characteristics of these photocatalytic nanoparticles, physicochemical characterizations have been performed using TEM, XRD, UV-Vis and FTIR. The rheological behavior of this nanofluid was also analyzed in the future perspective of the practical use of the suspension in wastewater treatment. These viscometric analyses show that the nanofilled suspension has a Newtonian behavior similar to the carrier liquid alone because of the small flow modification introduced by the gadolinium nanoparticles which remain well dispersed in the suspension.

Acknowledgments

We warmly thank Christelle Blavignac from the CICS (Centre d'Imagerie Cellulaire Santé) Clermont Auvergne University for the transmission electronic microscopy (TEM) characterization of the Gd_2O_3 nanoparticles.

References

1. Baskaran Chinnasamy. Mapping of quantitative analysis of research trend in nanomaterials. Materials Today: Proceedings. 2022; 49: 2922-2927.
2. Shumaila Ibraheem, Ghulam Yasin, Rashid Iqbal, et al. Silicon-based nanomaterials for energy storage. In Micro and Nano Technologies, Silicon-Based Hybrid Nanoparticles. 2022; 103-124.
3. Hilal Peçenek, Sevda Yetiman, Fatma Kılıç Dokan, et al. Effects of carbon nanomaterials and MXene addition on the performance of nitrogen doped MnO_2 based supercapacitors, Ceramics International. 2022; 48: 7253-7260.
4. Dhésmon Lima, Ariane Ribicki, Luana Gonçalves, et al. Nanoconjugates based on a novel organic-inorganic hybrid silsesquioxane and gold nanoparticles as hemocompatible nanomaterials for promising biosensing applications. Colloids and Surfaces B: Biointerfaces. 2022; 213: 112355.
5. Hazel O Simila, Aldo R. Boccaccini. Sol-gel bioactive glass containing biomaterials for restorative dentistry: A review. Dental Materials. 2022.
6. Young-Eun Choe, Yu-Jin Kim, Se-Jeong Jeon, et al. Investigating the echanophysical and biological characteristics of therapeutic dental cement incorporating copper doped bioglass nanoparticles. Dental Materials. 2022; 38: 363-375.
7. Hyder A, Jamil AB, Muhammad Nawaz, et al. Identification of heavy metal ions from aqueous environment through gold, Silver and Copper Nanoparticles: An excellent colorimetric approach. Environmental Research. 2022; 205: 112475.
8. Hamdullah Seckin, Rima Nour Elhouda Tiri, Ismet Meydan, et al. An environmental approach for the photodegradation of toxic pollutants from wastewater using Pt–Pd nanoparticles: Antioxidant, antibacterial and lipid peroxidation inhibition applications. Environmental Research. 2022; 208: 112708.
9. Anderson do Espirito Santo Pereira, Jhones Luiz de Oliveira, Susilaine Maira Savassa, et al. Lignin nanoparticles: New insights for a sustainable agriculture. Journal of Cleaner Production. 2022; 345: 131145.
10. Katarzyna Dziergowska, Izabela Michalak, Katarzyna Chojnacka, et al. The role of nanoparticles in sustainable agriculture. Smart Agrochemicals for Sustainable Agriculture. Academic Press. 2022; 225-278.
11. Anna Pajor-Świerzy, Krzysztof Szczepanowicz, Alexander Kamyshny, et al. Metallic core-shell nanoparticles for conductive coatings and printing. Advances in Colloid and Interface Science. 2022; 299: 102578.
12. Naharuddin NZA, Abu Bakar MH, Sadrolhosseini AR, et al. Pulsed-laser-ablated gold-nanoparticles saturable absorber for mode-locked erbium-doped fiber lasers. Optics & Laser Technology. 2022; 150: 107875.
13. Disha Iyengar, Katyayani Tatiparti, Navnath SG, et al. Nanomedicine for overcoming therapeutic and diagnostic challenges associated with pancreatic cancer. Drug Discovery Today. 2022.
14. Chelsea RT, Zlatko Kopecki, Anthony Wignall, et al. Liquid crystal nanoparticle platform for increased efficacy of cationic antimicrobials against biofilm infections. Nanomedicine: Nanotechnology, Biology and Medicine. 2022; 42: 102536.
15. Yanjun Du, Xiong Xu, Quanzhen Liu, et al. Identification of organic pollutants with potential ecological and health risks in aquatic environments: Progress and challenges. Science of the Total Environment. 2021; 806: 150691.
16. Marut Jain, Sadaf Aiman Khan, Komal Sharma, et al. Current perspective of innovative strategies for bioremediation of organic pollutants from wastewater. Bioresource Technology. 2022; 344: 126305.
17. Shubham Sutar, Prasanna Patil, Jyoti Jadhav. Recent advances in biochar technology for textile dyes wastewater remediation: A review. Environmental Research. 2022; 209: 112841.
18. Rania Al-Tohamy, Sameh SA, Fanghua Li, et al. A critical review on the treatment of dye-containing wastewater: Ecotoxicological and health concerns of textile dyes and possible remediation approaches for environmental safety. Ecotoxicology and Environmental Safety. 2022; 231: 113160.
19. Shubham Sutar, Prasanna Patil, Jyoti Jadhav. Recent advances in biochar technology for textile dyes wastewater remediation: A review. Environmental Research. 2022; 209: 112841.
20. Zaid HJ, Shahlaa Esmail Ebrahim. Recent advances in

nano-semiconductors photocatalysis for degrading organic contaminants and microbial disinfection in wastewater: A comprehensive review. Environmental Nanotechnology, Monitoring & Management. 2022; 17: 100666.

21. Amar RS, Pratik SD, Madhuri AB, et al. In-situ synthesis of metal oxide and polymer decorated activated carbon-based photocatalyst for organic pollutants degradation. Separation and Purification Technology. 2022; 286: 120380.
22. Keerthana SP, Yuvakkumar R, Ravi G, et al. Fabrication of Ce doped TiO_2 for efficient organic pollutants removal from wastewater. Chemosphere, 2022; 293: 133540.
23. Shan-Jiang Wang, Xiao-Yang Zhang, Dan Su, et al. Enhanced photocatalytic reactions via plasmonic metal-semiconductor heterostructures combing with solid-liquid-gas interfaces. Applied Catalysis B: Environmental. 2022; 306: 121102.
24. Jiratchaya Ayawanna, WahTzu Teoh, Sanyalak Niratisairak, et al. Gadolinia-modified ceria photocatalyst for removal of lead (II) ions from aqueous solutions. Materials Science in Semiconductor Processing. 2015; 40: 136-139.
25. Aditya MN, Thangapandi Chellapandi, Krishna Prasad G, et al. Biosynthesis of rod shaped Gd_2O_3 on g-C_3N_4 as nanocomposite for visible light mediated photocatalytic degradation of pollutants and RSM optimization. Diamond and Related Materials. 2022; 121: 108790.
26. Hang Liu, Guoxiu Wang, Chengyin Wang. Photocatalytic advanced oxidation processes for water treatment: recent advances and perspective. Chemistry - An Asian Journal. 2020.
27. Sagar Panwar, Gaurav KU, Purohit LP. Gd-doped ZnO: TiO_2 heterogenous nanocomposites for advance oxidation process. Materials Research Bulletin. 2022; 145: 111534.
28. Fei Li, Guo-Jun Zhang, Hiroya Abe. Low-temperature synthesis of high-entropy (Mg*0.2*Co*0.2*Ni*0.2*Cu*0.2*Zn*0.2*) O nanoparticles via polyol process. Open Ceramics. 2022; 9: 100223.
29. Soumitra Das, Girija KG, Debnath AK, et al. Enhanced NO_2 and SO_2 sensor response under ambient conditions by polyol synthesized Ni doped SnO_2 nanoparticles. Journal of Alloys and Compounds. 2021; 854: 157276.
30. Xiao Li, Cuimiao Zhang, Xiaomeng Jia, et al. Facile synthesis and size-dependent luminescence of gadolinium compounds with multiform morphologies and tunable particle sizes. Journal of Luminescence. 2021; 239: 118339.
31. Xiao Li, Jianru Wang, Ziman Yu, et al. Well-defined Gd(OH)CO_3, $Gd_2O(CO_3)_2 \cdot H_2O$, and Gd_2O_3 compounds with multiform morphologies and adjustable particle sizes: Synthesis, formation process, and luminescence properties. Colloids and Surfaces A: Physicochemical and Engineering Aspects. 2021; 624: 126834.
32. Fathyah Whba, Faizal Mohamed, Nur Ratasha Alia Rosli MD, et al. The crystalline structure of gadolinium oxide nanoparticles (Gd_2O_3-NPs) synthesized at different temperatures via X-ray diffraction (XRD) technique. Radiation Physics and Chemistry. 2021; 179: 109212.
33. Mudit Singh, Dipali Vadher, Vishwa Dixit, et al. Synthesis, optimization and characterization of zinc oxide nanoparticles prepared by sol–gel technique. Materials Today: Proceedings. 2022; 48: 690-692.
34. Anishur Rahman ATM, Krasimir Vasilev, Peter Majewski. Ultra small Gd_2O_3 nanoparticles: Absorption and emission properties. Journal of Colloid and Interface Science. 2011; 354: 592-596.
35. Xueliang Jiang, Lu Yu, Chu Yao, et al. Synthesis and Characterization of Gd_2O_3 Hollow Microspheres Using a Template-Directed Method. Materials. 2016; 9: 323.
36. The 4th International Conference on Water Resource and Environment (WRE 2018) IOP Conf. Series: Earth and Environmental Science. 2018; 191.
37. Syam Sundar L, Venkata Ramana E, Singh MK, et al. Viscosity of low volume concentrations of magnetic Fe_3O_4 nanoparticles dispersed in ethylene glycol and water mixture. Chemical Physics Letters. 2012; 554: 236-242.
38. Kazem Bashirnezhad, Shahab Bazri, Mohammad Reza Safaei, et al. Viscosity of nanofluids: A review of recent experimental studies. International Communications in Heat and Mass Transfer. 2016; 73: 114-123.
39. Omid Soltani, Mohammad Akbari. Effects of temperature and particles concentration on the dynamic viscosity of MgOMWCNT/ethylene glycol hybrid nanofluid: Experimental study. Physica E: Low-dimensional Systems and Nanostructures. 2016; 84: 564-570.
40. Di Wu, Chen Li, Dashuai Zhang, et al. Enhanced photocatalytic activity of Gd^{3+} doped TiO_2 and Gd_2O_3 modified TiO_2 prepared via ball milling method. Journal of Rare Earths. 2019; 37: 845-852.
41. Murugalakshmi M, Mamba G, Muthuraj V. A novel In_2S_3/Gd_2O_3 p-n type visible light-driven heterojunction photocatalyst for dual role of Cr (VI) reduction and oxytetracycline degradation. Applied Surface Science. 2020; 527: 146890.
42. Sugyeong jeon, Jeong-Won Ko, Weon-Bae Ko. Synthesis of Gd_2O_3 Nanoparticles and Their Photocatalytic Activity for Degradation of Azo Dyes. Catalysts. 2021; 11: 742.
43. Qazi Inamur Rahman, Musheer Ahmad, Sunil Kumar Misra, et al. Effective photocatalytic degradation of rhodamine B dye by ZnO nanoparticles. Materials Letters. 2013; 91: 170-174.
44. Nagaraja R, Nagaraju Kottam, Girija CR, et al. Photocatalytic degradation of Rhodamine B dye under UV/solar light using ZnO nanopowder synthesized by solution combustion route. Powder Technology. 2012; 215-216: 91-97.
45. Youji Li, Shuguo Sun, Mingyuan Ma, et al. Kinetic study and model of the photocatalytic degradation of rhodamine B (RhB) by a TiO_2-coated activated carbon catalyst: Effects of initial RhB content, light intensity and TiO_2 content in the catalyst. Chemical Engineering Journal. 2008; 142: 147-155.
46. Daneshvar N, Behnajady MA, Khayyat Ali Mohammadi M, et al. UV/H_2O_2 treatment of Rhodamine B in aqueous solution: Influence of operational parameters and kinetic modeling.

Desalination. 2008; 230: 16-26.

47. Ansaf V. Karim, Aydin Hassani, Paria Eghbali, et al. Nanostructured modified layered double hydroxides (LDHs)-based catalysts: A review on synthesis, characterization, and applications in water remediation by advanced oxidation processes. Current Opinion in Solid State and Materials Science. 2022; 26: 100965.
48. Soliu Oladejo Ganiyu, Shailesh Sable, Mohamed Gamal El-Din. Advanced oxidation processes for the degradation of dissolved organics in produced water: A review of process performance, degradation kinetics and pathway. Chemical Engineering Journal. 2022; 429: 132492.
49. Dhanalakshmi S, Senthil kumar P, Karuthapandian S, et al. Design of Gd_2O_3 nanorods: a challenging photocatalyst for the degradation of neurotoxicity chloramphenicol drug. Journal of Materials Science: Materials in Electronics. 2019; 30: 3744-3752.
50. Jyun-Hong Shen, Tzu-Hui Chiang, Cheng-Kuo Tsai, et al. Mechanistic insights into hydroxyl radical formation of Cu-doped ZnO/g-C_3N_4 composite photocatalysis for enhanced degradation of ciprofloxacin under visible light: Efficiency, kinetics, products identification and toxicity evaluation, Journal of Environmental Chemical Engineering. 2022; 10: 107352.
51. Shujing Liu, Chaojun Ren, Wenjun Li, et al. Novel Tb_2O_3/$Ag_2MO_2O_7$ heterojunction photocatalyst for excellent photocatalytic activity: In-built Tb^{4+}/Tb^{3+} redox center, proliferated hydroxyl radical yield and promoted charge carriers separation. Applied Surface Science. 2022; 584: 152531.